AIP | Journal of Applied Physics

Frequency-dependence of large-signal properties in lead-free piezoceramics

Robert Dittmer, Wook Jo, Emil Aulbach, Torsten Granzow, and Jürgen Rödel

Citation: Journal of Applied Physics **112**, 014101 (2012); doi: 10.1063/1.4730600
View online: http://dx.doi.org/10.1063/1.4730600
View Table of Contents: http://scitation.aip.org/content/aip/journal/jap/112/1?ver=pdfcov
Published by the AIP Publishing

Frequency-dependence of large-signal properties in lead-free piezoceramics

Robert Dittmer, Wook Jo,[a] Emil Aulbach, Torsten Granzow, and Jürgen Rödel
Institute of Materials Science, Technische Universität Darmstadt, Petersenstr. 23, 64287 Darmstadt, Germany

(Received 15 December 2011; accepted 26 April 2012; published online 2 July 2012)

The dependence of large signal properties of $(1-x)(0.81Bi_{1/2}Na_{1/2}TiO_3\text{-}0.19Bi_{1/2}K_{1/2}TiO_3)\text{-}xBi(Zn_{1/2}Ti_{1/2})O_3$ with $x = 0.02$, 0.03, and 0.04 on the measurement frequency was investigated for a wide range of frequencies from 0.1 Hz to 100 Hz. A significant frequency dispersion in the characteristic parameters representatively maximum and coercive values was denoted. On extension with the temperature dependent dielectric permittivity measurement, it was shown that the observed frequency dependence is primarily correlated with the dynamics of field-induced phase transition from a relaxor state to a long-range ferroelectric state. Increasing the substitutional disorder introduced by $Bi(Zn_{1/2}Ti_{1/2})O_3$ addition was demonstrated to pronounce the frequency dependence. It was proposed that the change be due to the increase in random fields and consequent dominance of ergodicity, based on the frequency-dependent hysteresis measurements at an elevated temperature above so-called induced-ferroelectric-to-relaxor transition temperature.
 [http://dx.doi.org/10.1063/1.4730600]

I. INTRODUCTION

Piezoelectric materials have a variety of applications because of their ability in coupling electric fields and mechanical strain.[1,2] Among these applications are ultrasound generation,[3] energy harvesting,[4,5] sensors,[6,7] and actuators.[8,9] However, a drawback is the incorporation of lead in most state-of-the-art materials such as $(1-x)Pb(Mg_{1/3}Nb_{2/3})O_3\text{–}xPbTiO_3$ (PMN-PT), $Pb(Zr_xTi_{1-x})O_3$ (PZT), or $Pb_{1-y}La_y(Zr_xTi_{1-x})O_3$ (PLZT), which creates an increasing conflict with the attempt to minimize the amount of lead in consumer products. Legislations like RoHS/WEEE (restriction of hazardous substances/waste electrical and electronic equipment[10,11]) that restrict the use of lead-containing materials triggered research to find lead-free alternatives. Bismuth-based ceramics such as $Bi_{1/2}Na_{1/2}TiO_3$ (BNT) and $Bi_{1/2}K_{1/2}TiO_3$ (BKT) denote promising starting points because of the resemblance of the Bi^{3+} ion with the Pb^{2+} ion in terms of electronic configuration, i.e., a $6s^2$ lone-pair configuration.[12–15] As BNT requires high switching fields and BKT is hard to fully densify by conventional sintering techniques, solid solutions of these materials were investigated.[16,17] It was found that compositions at the morphotropic phase boundary (MPB) of $(1-x)BNT\text{-}xBaTiO_3$ ($(1-x)BNT\text{-}xBT$, with $x = 0.06 \sim 0.07$) and $(1-x)BNT\text{-}xBKT$ (with $x = 0.16 \sim 0.2$) offer enhanced electrical properties.[18–20] *In situ* diffraction studies revealed that the morphotropic BNT-BT and BNT-BKT undergo an irreversible phase transition at a certain electric field, where the initial pseudocubic symmetry is altered towards tetragonal or tetragonal and rhombohedral mixture.[15,21,22]

One focal point of international research efforts is a further improvement of these materials. One way to achieve this is compositional variation by chemical modifications. Zhang *et al.*[23] showed that the introduction of $(K_{0.5}Na_{0.5})NbO_3$ (KNN) to 0.94BNT-0.06BT significantly alters the large and small signal properties. They reported that the addition of KNN makes the material exhibit a notably large normalized strain (S_{max}/E_{max}, where S_{max} and E_{max} denote the maximum strain and electric field, respectively) with the small signal piezoelectric coefficient decreasing rapidly, when E_{max} exceeds 6 kV/mm. Follow-up studies revealed that the large S_{max}/E_{max} happens when the remanent state is absent even after electrical poling,[24] and the absence of the remanent state is related to the high temperature polymorph.[25] Jo *et al.*[26] proposed a reversible electric-field-induced phase transition between a "non-polar" and ferroelectric phase as the underlying mechanism.

Hinterstein *et al.*[27] demonstrated for 0.92BNT-0.06BT-0.02KNN that the previously proposed reversible phase transition involves a symmetry change, i.e., from a tetragonal phase with an extremely small tetragonality of 1.0003 to a rhombohedral phase with a noticeable distortion. This phase transition was suggested as the cause for the peculiar large-strain behavior. Later on, other authors have shown that a variety of other dopants are also capable of introducing this large-strain behavior such as Al, Hf, and Zr.[28–30] Although specifics like the magnitude of S_{max}/E_{max} are varying among the multitude of compositions, the basic characteristics under high fields are very similar. This can be rationalized as the base-material BNT itself is a relaxor where chemical modification with foreign elements would influence merely the relaxor features with a different degree of random fields.[31]

One aspect that has been overlooked is the frequency-dependence of both strain and polarization hysteresis. This is, however, a crucial aspect if final applications are considered. Characterization of hystereses in academic research is often performed at around 1 Hz or below. In contrast, actuators as utilized, for example, in piezoelectric fuel injectors usually operate at frequencies of several tens or hundreds of hertz.[32–35] This discrepancy in applied frequencies raises the question whether the above mentioned lead-free large-strain materials are subject to a significant frequency-dependence and whether they are still able to deliver high strains even at

[a]Author to whom correspondence should be addressed. Electronic mail: jo@ceramics.tu-darmstadt.de.

elevated frequencies. More importantly, the physical reason for the large strain behavior is not yet fully clarified. Therefore, a compositional study of the frequency dependence in P(E) and S(E) could deliver further insight into the underlying mechanisms in this group of materials.

Other than in lead-free materials, there are some reports on frequency-dependence of strain and polarization hysteresis for conventional piezoceramics. Chen and Viehland[36] reported on P(E) and S(E) loops as a function of frequency for the soft ferroelectric 0.7PMN-0.3PT at different maximum fields. For field amplitudes below the coercive field (E_c), they found a strong relaxation in polarization with maximum polarization (P_{max}) and remanent polarization (P_{rem}) increasing with decreasing frequencies. The field-induced strain accordingly mirrored polarization behavior. Maximum fields beyond the coercive field yielded ferroelectric hysteresis loops where P_{rem} and P_{max} as well as S_{rem} and S_{max} were virtually frequency-independent. However, E_c and the negative strain (S_{neg}) showed notable variance with both values, increasing with increasing driving frequencies, which lead to the random-field model.[37] Gao *et al.*[38] compared frequency-dependent polarization loops of a soft and a hard PZT with those of PZT-Pb(Sb, Mn)O_3 and also found relaxational polarization behaviors in all three materials. On the other hand, Zhang *et al.*[39] reported the frequency-dependent strains of a relaxor ferroelectric PLZT 9/65/35. They noted a decreasing maximum strain with increasing frequency, which was later confirmed by Shrout and Jang.[40] There are more reports on the frequency dependence of the polarization loop in classical lead-containing materials for both bulk and thin film materials.[41–45] For lead-free piezoelectrics, however, no systematic investigation on the effect of different driving frequencies is available in the literature yet.

In this work, we present a study of frequency-dependent high-field behavior of strain (S(E)) and polarization (P(E)) from 0.1 Hz to 100 Hz for lead-free 0.81BNT-0.19BKT, the composition of which lies within the MPB region.[46] We introduced a mixed B-site occupancy of Zn^{2+} and Ti^{4+} by incorporating $BiZn_{1/2}Ti_{1/2}O_3$ (BZT). The BZT-content in the given chemical formula, (1−x)(0.81BNT-0.19BKT)-xBZT, was varied from x = 0.02 to 0.04, because they all exhibit a field-induced phase transition from a relaxor to a long-range-ordered phase but the nature of phase transition changes from an irreversible to a reversible one with increasing x. As noted, this change is featured by the appearance of a large strain with the remanent strain diminishing. We show that the large-field properties are strongly dependent on the measurement frequency and the dependence is more pronounced with increasing x. The underlying mechanism for the frequency dependence was further enlightened by the observations compared with the frequency-dependent P(E) and S(E) of 0.98(0.81BNT-0.19BKT)-0.02BZT at 90 °C. It is important to note that every single S(E) and P(E) measurement was performed from the virgin state. Hence, more information can be drawn from these measurements, as some important features occur exclusively in the very first half-cycle. The definition for the parameters used in the current manuscript is illustrated in Fig. 1.

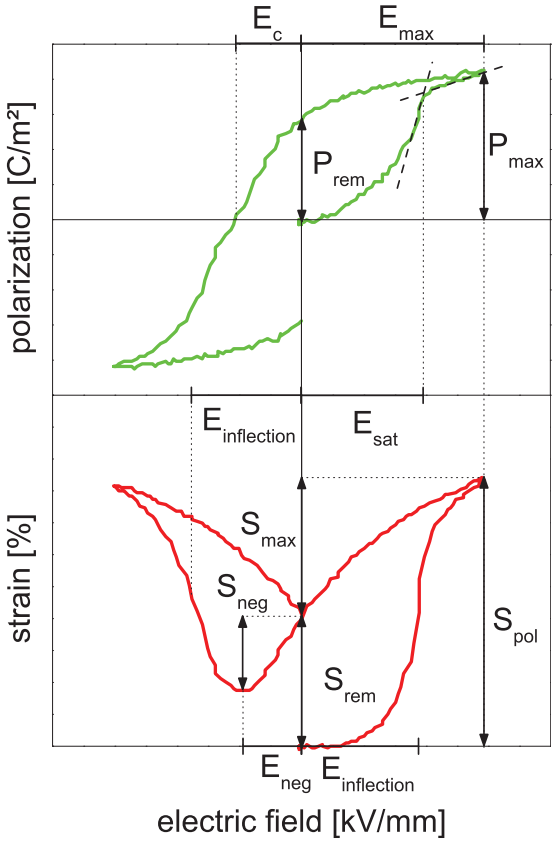

FIG. 1. Schematic illustrating characteristic parameters derived from S(E) and P(E) curves.

II. MATERIALS AND METHODS

A. Sample preparation

The ceramic powders of the composition (1−x)(0.81BNT-0.19BKT)-xBZT with x = 0.02, 0.03, and 0.04 (in the following, termed as 2BZT, 3BZT, and 4BZT, respectively) were produced by the mixed oxide route from reagent grade raw powders (all Alfa Aesar GmbH & Co. KG, Karlsruhe, Germany) Bi_2O_3 (99.975% purity), $NaCO_3$ (99.5%), TiO_2 (99.9%), K_2CO_3 (99.0%), and ZnO_2 (99.99%). Details of the powder processing are given elsewhere.[47] The samples were shaped by uniaxial pressing using a pressing die of 10 mm in diameter with subsequent cold-isostatic pressing at 300 MPa. The pellets thus prepared were sintered for 3 h at 1100 °C in covered alumina crucibles. To minimize loss of volatile elements, the samples were covered in atmospheric powder of the respective composition. Sintered pellets were ground and polished down to 0.8 mm in thickness and electroded with a silver paste that was burnt in at 400 °C.

B. Electrical measurements

The polarization and strain measurements were conducted in a modified Sawyer-Tower setup with a measurement capacitance of 15 μF. Using an optical displacement sensor (Philtec, Inc., Annapolis, MD, USA), the accessible frequency range for S(E) was greatly increased in comparison to conventional linear variable differential transformer (LVDT) sensors. Therefore, P(E) and S(E) loops could be

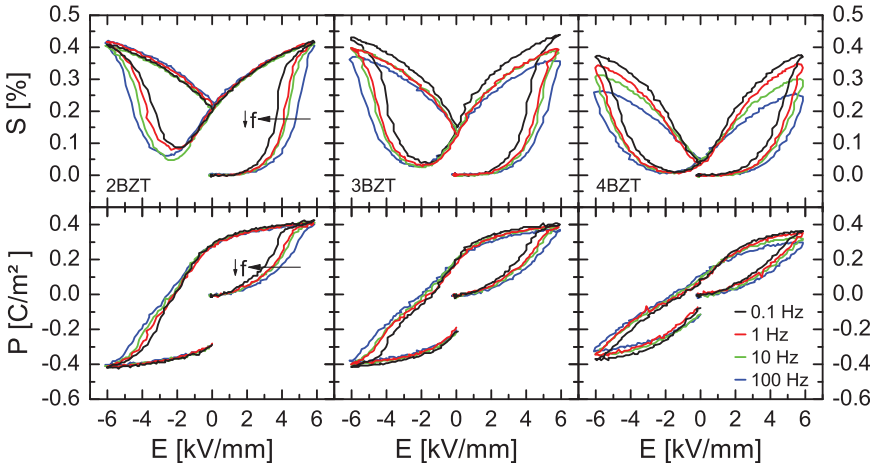

FIG. 2. Compositional evolution of frequency-dependent field-induced strain S(E) and polarization P(E) with increasing Zn^{2+}-content.

recorded at 0.1 Hz, 1 Hz, 10 Hz, and 100 Hz, covering four orders of magnitude. To obtain virgin curves, each sample was wrapped in aluminum foil and annealed for 10 min at 400 °C on a heating stage. To prevent thermal shock and cracking, the samples were cooled down to about 100 °C before being removed from the heating stage. Temperatures were double-checked with a thermocouple, and the piezoelectric charge constant was checked with a Berlincourtmeter (Sinoceramics Inc., Shanghai, China). To obtain P(E) and S(E) loops at elevated temperatures, a temperature control was integrated into an oil bath, consisting of a resistive heating element, a temperature-controller, and a thermocouple immersed in the oil bath very close to the sample. Relative dielectric permittivity and loss factor were measured in a Nabertherm LE4/11/R6 box furnace (Nabertherm GmbH, Lilienthal, Germany) with a custom-made sample holder and an HP 4284 A impedance analyzer (Hewlett-Packard Co., Palo Alto, CA, USA) at a heating rate of 2 K/min. Prior to this measurement, the samples were poled in an oil bath at room temperature for 10 min under an electric field of 6 kV/mm.

III. RESULTS

A. Room temperature measurements

Figure 2 presents the large-signal polarization and strain loops for the three compositions at 0.1 Hz, 1 Hz, 10 Hz, and 100 Hz. The general characteristic of P(E) and S(E) changes significantly with increasing substitution of Zn^{2+} for B-site. Similar to morphotropic BNT-BKT or BNT-BT, 2BZT has a high P_{rem} of 0.27 C/m^2 and a high S_{rem} of 0.21%. Both values diminish with further addition of Zn^{2+}, eventually giving rise to the aforementioned large-strain behavior in 4BZT, which features a large strain during unipolar loading. The composition 3BZT marks an intermediate state with decreased S_{rem} of 0.13% and P_{rem} of 0.17 C/m^2.

A salient feature is the distinct frequency-dependence that is found for all three compositions, albeit with significantly different aspects. In all compositions, the relevant field parameters, i.e., the coercive field (E_c), the field defined by the maximum slope in the S(E) curve ($E_{inflection}$), as well as the field for maximum negative strain (E_{neg}), increase with increasing frequency as illustrated in Fig. 3. Moreover, S_{rem} and P_{rem} remain unchanged in all samples, but in 3BZT and 4BZT, the poling strain (S_{pol}) is very sensitive to frequency changes as depicted in Fig. 4. Consequently, the normalized strain S_{max}/E_{max} drops notably when the frequency is increased. In the case of 4BZT, S_{max}/E_{max} decreases from 580 pm/V for 0.1 Hz down to 340 pm/V for 100 Hz, which denotes a drop by as large as ~41%.

B. Measurements at elevated temperatures

Measurements of dielectric properties from room temperature up to 400 °C for frequencies from 1 kHz up to 1 MHz are presented in Fig. 5. All three compositions exhibit very similar behavior in $\varepsilon_{r,33}(T)$ and $\tan\delta(T)$. The dielectric permittivity features a broad maximum at around 300 °C with a low-temperature shoulder. The frequency dispersion

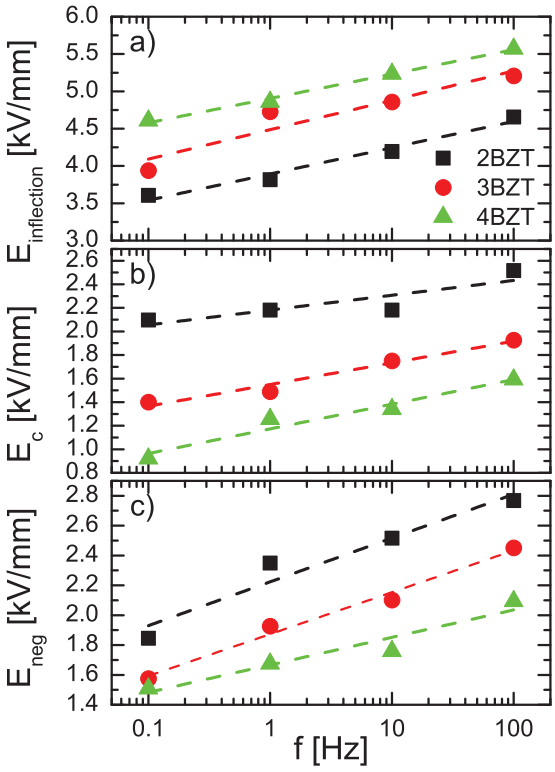

FIG. 3. Characteristic fields determined from frequency dependent measurements for 2BZT, 3BZT, and 4BZT: (a) field of maximum slope in S(E) curve $E_{inflection}$, (b) coercive field E_c, and (c) field of negative strain E_{neg}.

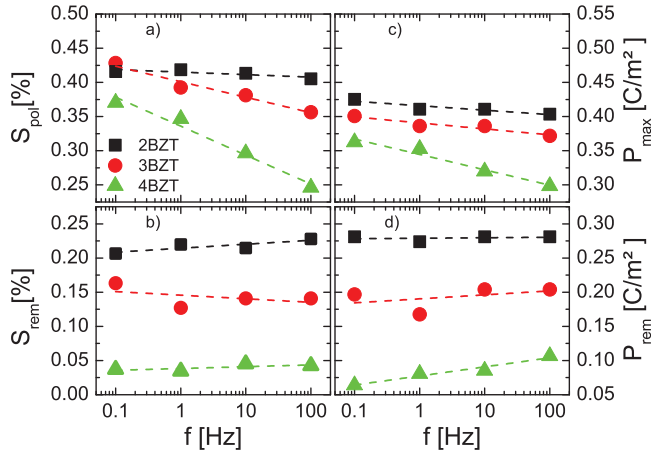

FIG. 4. Strain and polarization parameters derived from the frequency dependent measurements for 2BZT, 3BZT, and 4BZT: (a) poling strain, S_{pol}, (b) remanent strain, S_{rem}, and (c) maximum polarization, P_{max}, remanent polarization, P_{rem}.

in the low-temperature region of $\varepsilon_{r,33}$ is also reflected in tanδ, which is an indication for relaxor behavior.[31] The nearly frequency-independent first peak in tanδ has been taken in the literature to characterize the depolarization temperature.[18] Recent work contrasting temperature dependence of dielectric permittivity, depolarization current, and piezoelectric coefficient demonstrated that the temperature found using tanδ is above the true depolarization temperature.[47] This was ascertained using further field dependence together with temperature dependence of permittivity and depolarization current.[48] Here, we are fundamentally interested in ferroelectric–relaxor transitions and determine the peak in tanδ in order to quantify the ferroelectric–relaxor transition ($T_{F\text{-}R}$).[31,48] This temperature decreases with increasing Zn^{2+}-content from 55 °C in 2BZT to 45 °C in 3BZT. Eventually, no transition is observed for 4BZT above 25 °C. The general trend suggests that the ferroelectric—relaxor transition lies below room temperature.

Figure 6 presents the field-induced strain and polarization of 2BZT at 90 °C. This temperature was chosen because it lies well above $T_{F\text{-}R}$. It is obvious that the increase in temperature has a dramatic effect on the strain response. First, the remanent strain, S_{rem} drops from about 0.2% down to about 0.1%. Moreover S_{rem} appears to vary with frequency, whereas it is invariant at room temperature. The difference in S_{rem} with frequency, however, is only pronounced between 0.1 Hz and 1 Hz. The change in S_{rem} above 1 Hz is so small and non-systematic that it may be induced by temperature fluctuation and consequent thermal drifting effects. In contrast to S_{rem} and unlike the room-temperature behavior of 2BZT, the maximum strain during poling (S_{pol}) strongly depends on frequency: the sample delivers almost 0.2% less strain at the frequency of 100 Hz in comparison to 100 mHz. Nonetheless, the maximum strain at 90 °C is significantly larger than that at room temperature for all frequencies due to the drop in the remanent strain. Consequently, S_{max}/E_{max} is increased from virtually frequency-independent 350 pm/V at room temperature to 445 pm/V at 100 Hz and 606 pm/V at 100 mHz. Therefore, 2BZT provides a strain response at 90 °C that is to some extent comparable to the room-temperature response of 4BZT, which was also shown to exhibit frequency-dependent large-strain behavior. Compared to room temperature, the P(E) loop at 90 °C is notably slimmer and slightly pinched, which again resembles the compositional evolution illustrated in Fig. 2. The remanent polarization decreased from about 0.27 C/m^2 down to 0.12 C/m^2 with the maximum polarization virtually unchanged at about 0.42 C/m^2. For the 1 Hz measurement, this corresponds to a back-switching ($P_{max}-P_{rem}$)/P_{max} of 33% at room temperature and 73% at 90 °C. That value is higher than the 57% back-switching observed in 3BZT at 1 Hz and close to the 78% found for the same frequency in 4BZT. Despite the similarities between 2BZT at 90 °C and 4BZT at room temperature, there are some noticeable differences. The maximum polarization in 2BZT is frequency-independent whereas it

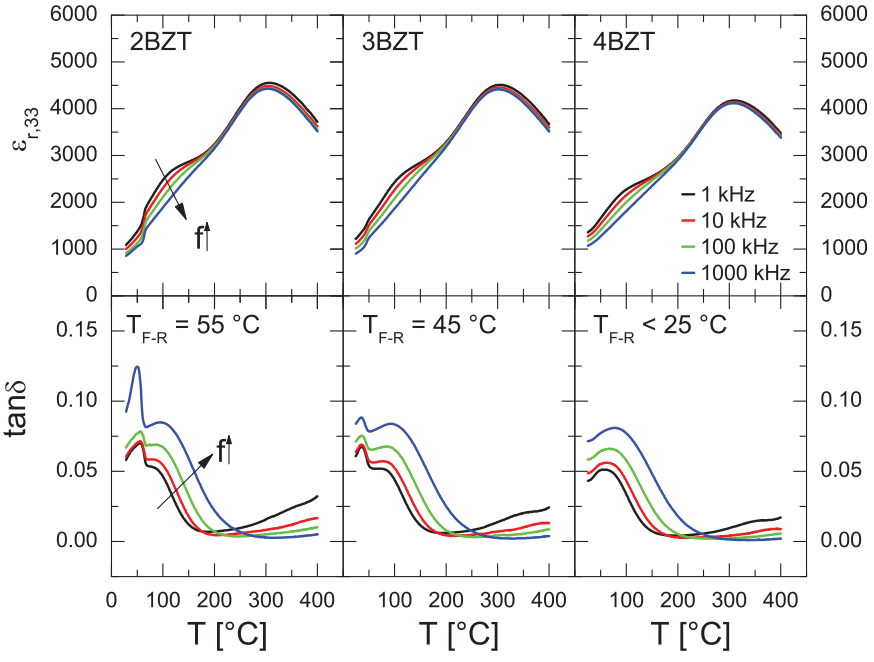

FIG. 5. Relative dielectric permittivity $\varepsilon_{r,33}$ and loss factor tanδ of poled samples at various frequencies.

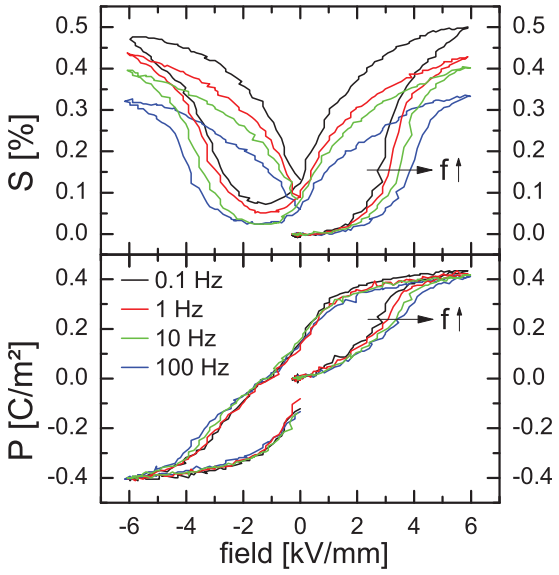

FIG. 6. Frequency-dependent strain S(E) and polarization P(E) of 2BZT at 90 °C.

varies in 4BZT, if only to a small extent. Moreover, a distinguishable field, E_{sat} can be determined in 2BZT where the polarization saturates during the first half-cycle at room temperature and 90 °C. At both temperatures, E_{sat} is frequency-dependent, shifting to higher electric fields with increasing frequency. This saturation field in P(E) correlates with the $E_{inflection}$ in the S(E) curve, i.e., a sharp increase in strain is observed just below E_{sat}. Figure 7 illustrates this correlation. It is obvious that both E_{sat} and $E_{inflection}$ decrease for all frequencies at the elevated temperature. For example, E_{sat} at 1 Hz is reduced from 4.6 kV/mm at room temperature down to 3.6 kV/mm at 90 °C. In 4BZT, P(E) does not saturate and, therefore, no E_{sat} can be defined.

IV. DISCUSSION

We have found significant influences of measurement frequency on large-signal behaviors, ranging from 0% to 41% in S_{max}/E_{max} depending on extension of ferroelectric order. In contrast, lead-containing materials often show no

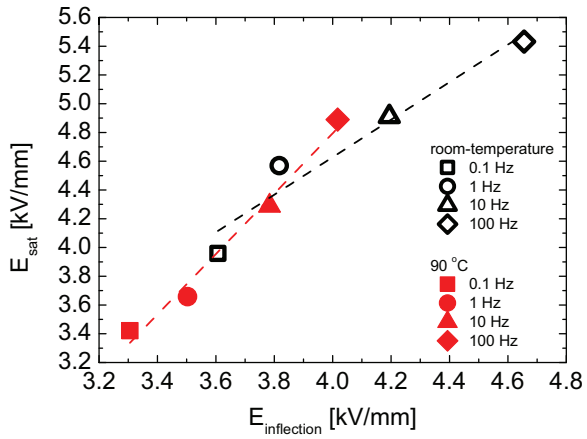

FIG. 7. Correlation of E_{sat} determined from P(E) and $E_{inflection}$ determined from S(E) for 2BZT at room-temperature and 90 °C.

such pronounced frequency dependence of strain as demonstrated for soft PZT or 70-PMN-30PT.[36–38] On the other hand, the relaxor material PLZT 9/65/35 features a strain response that is likewise dependent on frequency where S_{max} decreases by about 20% when the driving frequency is increased from 1 Hz to 100 Hz.[39]

To explain the evolution of S(E) and P(E) illustrated in Fig. 2, we therefore suggest that BNT-BKT-BZT is a relaxor ferroelectric that undergoes a field-induced transition from a relaxor to a state with a ferroelectric long-range order.[46] This transition is highly dependent on the applied field, but also on composition, frequency, and temperature. We assume that below a field limit, polar nanoregions (PNRs) exist, but ferroelectric macrodomains do not. Upon passing a critical field, a transition with the development of ferroelectric long-range order occurs. With a little mixed B-site occupation, as in 2BZT, the field required to induce the phase transition is comparably low. Therefore, 2BZT can be poled at moderate electric fields; hence, appears ferroelectric under high fields and possesses a sizable small signal d_{33} of 139 pC/N. In an earlier report, we found via high-energy *in situ* XRD under electric field that E_{sat} is correlated with the critical field, where a long-range order is established and non-cubic distortion is detected.[46] For 2BZT, this means that the transition takes place in the range of E_{sat} around 4 kV/mm at 100 mHz. The P(E) loop of 2BZT shows practically no constriction, which implies that the induced ferroelectric order is comparably stable on the removal of electric field. This observation suggests that the transition is from a non-ergodic relaxor state to a ferroelectric.

Increasing the dopant content progressively impedes the creation of ferroelectric long-range order as indicated by E_{sat} which increased from 4 kV/mm in 2BZT to 4.6 kV/mm in 3BZT at 100 mHz. This result can be rationalized by the higher fraction of Zn^{2+} ions that occupy the B-site of perovskite lattice in 3BZT and cause a higher degree of disorder. This increased substitutional charge disorder implicates an augmentation of random fields. Consequently, the establishment of a long-range order is restrained. In 4BZT, no saturation polarization is reached with fields up to 6 kV/mm, i.e., the transition is even more impeded by the increased Zn^{2+} content. During the reduction of electric field, the induced long-range order collapses and consequently P_{rem} and S_{rem} are diminished, meaning that the relaxational behavior is due to a series of transitions from an ergodic relaxor to an induced ferroelectric and back to the ergodic relaxor. However, the non-zero remanence suggests that the long-range order still persists in some volume fraction of the samples. This can also be grasped by the pinched polarization loop in 3BZT and 4BZT, which indicates that at least a part of the induced long-range order is not stable in the absence of external field.

A similar behavior has been ascertained in field-dependent transmission electron microscopy on the ergodic relaxor 0.91BNT-0.06BT-0.03KNN, where ferroelectric domains appeared and disappeared with increasing and decreasing electric field, respectively.[49] Similarly, the reversible phase transition has been demonstrated both with synchrotron as well as with neutron diffraction on 0.92BNT-0.06BT-

0.02KNN.[27] In the case of 0.92BNT-0.06BT-0.02KNN and 0.91BNT-0.06BT-0.03KNN, ferroelectric domains appear with crystallographic symmetry changing, which could be interrogated with diffraction techniques applied.

The same argument applies to the high-temperature measurement presented in Fig. 6, where it is not the substitutional charge disorder but the thermal excitation that causes the instability of the ferroelectric long-range order. Ultimately, the large signal behavior of 2BZT at 90 °C mimics that of 4BZT at room temperature, i.e., a transition takes place from ergodic relaxor to a ferroelectric. Upon removal of the electric field, the majority of the long-range order collapses, and the ergodic relaxor state is recovered with only a minute remanence. The frequency dependence of strain and polarization in 2BZT underpins the assumption of a transition from non-ergodic to a long-range ferroelectric state. Since E_{sat} depends on frequency, it is concluded that the field-induced phase transition is also frequency-dependent in a sense that the transition is triggered at lower fields for lower frequencies. The observed time dependence suggests that the mechanism of the transition be associated with coalescence of PNRs. Under the electric field, the PNRs start to grow in size until they eventually overcome the existing random field to form ferroelectric domains. In the case of 2BZT, the maximum field of 6 kV/mm is sufficient for the material to be fully converted into the ferroelectric state. Therefore, S_{max} and P_{max} are virtually frequency-independent. This is, however, not true at lower fields as evidenced by a significant frequency dispersion of S(E), e.g., at 4 kV/mm, where strain during the first half-cycle is 0.3% at 100 mHz and only 0.07% at 100 Hz. The physical reason is the incomplete transition into a long-range-ordered state.

Other than in 2BZT, the frequency dispersion persists in 3BZT and 4BZT up to the maximum field of 6 kV/mm. As presented in Fig. 4, the frequency dispersion increases with increasing Zn^{2+}-content. This observation is in agreement with the assumption of a material that exhibits ergodicity to some extent. Because of the weakly correlated PNRs, there is a distribution of relaxation times. Consequently, the properties under field are highly frequency-dependent. The same frequency dependence is introduced in 2BZT when the sample is heated beyond T_{F-R}, which is associated with a transition from the nonergodic to the ergodic relaxor state.

V. SUMMARY AND CONCLUSION

We presented a compositional study of frequency-dependent field-induced strain and polarization in lead-free morphotropic BNT-BKT doped with Zn^{2+} on the B-site of the perovskite lattice. It was found that the field-induced phase transition does not only depend on field and composition but also frequency and temperature. It was shown that the higher the frequencies are, the higher the field for the phase transition to take place, which is a clear evidence that the transition is time-dependent. For a low content of B-site dopants (as in 2BZT), the coercive field in the P(E) loop demonstrates very little frequency-dependence, which is in contrast to lead-containing soft ferroelectrics. At room temperature, both maximum strain and polarization are likewise frequency-independent within the considered frequency range from 100 mHz to 100 Hz. For temperatures beyond T_{F-R}, however, it was shown that frequency dispersion emerges, most likely due to the appearance of ergodicity.

For a higher degree of mixed B-site occupation, the maximum strain is strongly frequency-dependent even at room temperature, where the formation of ferroelectric long-range order is suggested being impeded by the increased Zn^{2+} content. The normalized strain S_{max}/E_{max} was shown to decrease by about 40% when the frequency is increased from 100 mHz to 100 Hz. These high frequencies, however, are often required for actuator applications. Consequently, a clear understanding of the described frequency dependence is crucial for the potential utilization of lead-free materials.

ACKNOWLEDGMENTS

This work was financially supported by the Deutsche Forschungsgemeinschaft (DFG) under SFB 595.

[1]D. Damjanovic, Rep. Prog. Phys. **61**, 1267 (1998).
[2]B. Jaffe, W. R. Cook, and H. Jaffe, *Piezoelectric Ceramics* (Academic, London, 1971), Vol. 115.
[3]B. W. Drinkwater and P. D. Wilcox, NDT & E Int. **39**, 525 (2006).
[4]S. R. Anton and H. A. Sodano, Smart Mater. Struct. **16**, R1 (2007).
[5]S. P. Beeby, M. J. Tudor, and N. M. White, Meas. Sci. Technol. **17**, R175 (2006).
[6]P. B. Luppa, L. J. Sokoll, and D. W. Chan, Clin. Chim. Acta **314**, 1 (2001).
[7]P. Leonard, S. Hearty, J. Brennan, L. Dunne, J. Quinn, T. Chakraborty, and R. O'Kennedy, Enzyme Microb. Technol. **32**, 3 (2003).
[8]H. S. Tzou, H. J. Lee, and S. M. Arnold, Mech. Adv. Mater. Struct. **11**, 367 (2004).
[9]E. K. Akdogan, M. Allahverdi, and A. Safari, IEEE Trans. Ultrason. Ferroelectr. Freq. Control **52**, 746 (2005).
[10]The European Parliament and the Council of the European Union, Off J. Eur. Union **46**, 19 (2003).
[11]The European Parliament and the Council of the European Union, Off. J. Eur. Union **46**, 24 (2003).
[12]M. R. Suchomel, A. M. Fogg, M. Allix, H. J. Niu, J. B. Claridge, and M. J. Rosseinsky, Chem. Mater. **18**, 4987 (2006).
[13]G. A. Smolenskii and A. I. Agranovskaya, Sov. Phys. Solid State **1**, 1429 (1960).
[14]G. A. Smolenskii, V. A. Isupov, A. I. Agranovskaya, and N. N. Krainik, Sov. Phys. Solid State **2**, 2651 (1961).
[15]A. J. Royles, A. J. Bell, A. P. Jephcoat, A. K. Kleppe, S. J. Milne, and T. P. Comyn, Appl. Phys. Lett. **97**, 132909 (2010).
[16]J. Rödel, W. Jo, K. T. P. Seifert, E. M. Anton, T. Granzow, and D. Damjanovic, J. Am. Ceram. Soc. **92**, 1153 (2009).
[17]T. Takenaka and H. Nagata, J. Eur. Ceram. Soc. **25**, 2693 (2005).
[18]T. Takenaka, K. Maruyama, and K. Sakata, Jpn. J. Appl. Phys., Part 1 **30**, 2236 (1991).
[19]Y. Hiruma, H. Nagata, and T. Takenaka, J. Appl. Phys. **104**, 124106 (2008).
[20]A. Sasaki, T. Chiba, Y. Mamiya, and E. Otsuki, "Dielectric and piezoelectric properties of $(Bi_{0.5}Na_{0.5})TiO_3$-$(Bi_{0.5}K_{0.5})TiO_3$ systems," Jpn. J. Appl. Phys., Part 1 **38**, p. 5564 (1999).
[21]J. E. Daniels, W. Jo, J. Rodel, and J. L. Jones, Appl. Phys. Lett. **95**, 032904 (2009).
[22]H. Simons, J. Daniels, W. Jo, R. Dittmer, A. Studer, M. Avdeev, J. Rödel, and M. Hoffman, Appl. Phys. Lett. **98**, 082901 (2011).
[23]S. T. Zhang, A. B. Kounga, E. Aulbach, H. Ehrenberg, and J. Rödel, Appl. Phys. Lett. **91**, 112906 (2007).
[24]S. T. Zhang, A. B. Kounga, E. Aulbach, T. Granzow, W. Jo, H. J. Kleebe, and J. Rödel, J. Appl. Phys. **103**, 034107 (2008).
[25]S. T. Zhang, A. B. Kounga, E. Aulbach, W. Jo, T. Granzow, H. Ehrenberg, and J. Rödel, J. Appl. Phys. **103**, 034108 (2008).

[26]W. Jo, T. Granzow, E. Aulbach, J. Rodel, and D. Damjanovic, J. Appl. Phys. **105**, 094102 (2009).
[27]M. Hinterstein, M. Knapp, M. Hölzel, W. Jo, A. Cervellino, and H. Ehrenberg, J. Appl. Crystallogr. **43**, 1314 (2010).
[28]A. Ullah, C. W. Ahn, A. Hussain, S. Y. Lee, H. J. Lee, and I. W. Kim, Curr. Appl. Phys. **10**, 1174 (2010).
[29]A. Hussain, C. W. Ahn, A. Ullah, J. S. Lee, and I. W. Kim, Jpn. J. Appl. Phys., Part 1 **49**, 041504 (2010).
[30]A. Hussain, C. W. Ahn, J. S. Lee, A. Ullah, and I. W. Kim, Sens. Actuators, A **158**, 84 (2010).
[31]W. Jo, S. Schaab, E. Sapper, L. A. Schmitt, H.-J. Kleebe, A. J. Bell, and J. Rödel, J. Appl. Phys. **110**, 074106 (2011).
[32]M. S. Senousy, F. X. Li, D. Mumford, M. Gadala, and R. K. N. D. Rajapakse, J. Intell. Mater. Syst. Struct. **20**, 387 (2009).
[33]M. S. Senousy, R. K. N. D. Rajapakse, D. Mumford, and M. S. Gadala, Smart Mater. Struct. **18**, 045008 (2009).
[34]F. Zunqiang, L. Jianfang, Y. Zhigang, and L. Jianqiao, in *Study on the Control of Precise Actuator with Piezoelectric Stack Pump* (2010), p. 738.
[35]S. Sherrit, B. Xiaoqi, C. M. Jones, J. B. Aldrich, C. J. Blodget, J. D. Moore, J. W. Carson, R. Goullioud, and B. Jau, in *Piezoelectric Stack Actuator Life Test* (2011), p. 1.
[36]Y. H. Chen and D. Viehland, Appl. Phys. Lett. **77**, 133 (2000).
[37]D. Viehland and Y. H. Chen, J. Appl. Phys. **88**, 6696 (2000).
[38]Y. Gao, K. Uchino, and D. Viehland, J. Appl. Phys. **92**, 2094 (2002).
[39]Q. M. Zhang, S. J. Jang, and L. E. Cross, J. Appl. Phys. **65**, 2807 (1989).
[40]T. R. Shrout and S.-J. Jang, *Relaxor Ferroelectrics for Electrostrictive Transducer*, in Quarterly Report Sep. 1991 - 31 Jan. 1992 Pennsylvania State Univ., University Park Materials Research Lab (1992).
[41]M. H. Lente, A. Picinin, J. P. Rino, and J. A. Eiras, J. Appl. Phys. **95**, 2646 (2004).
[42]Y. H. Chen, K. Uchino, and D. Viehland, J. Appl. Phys. **89**, 3928 (2001).
[43]R. Yimnirun, S. Wongsaenmai, S. Ananta, and Y. Laosiritaworn, Appl. Phys. Lett. **89**, 242901 (2006).
[44]X. F. Chen, X. L. Dong, N. B. Feng, H. C. Nie, F. Cao, G. S. Wang, Y. Gu, and H. L. He, Solid State Commun. **149**, 663 (2009).
[45]J. F. Scott, Integr. Ferroelectr. **12**, 71 (1996).
[46]R. Dittmer, W. Jo, J. Daniels, S. Schaab, and J. Rödel, J. Am. Ceram. Soc. **94**, 4283 (2011).
[47]E. M. Anton, W. Jo, J. Trodahl, D. Damjanovic, and J. Rödel, Jpn. J. Appl. Phys., Part 1 **50**, 055802 (2011).
[48]E. Sapper, S. Schaab, W. Jo, T. Granzow, and J. Rödel, J. Appl. Phys. **111**, 014105 (2012).
[49]J. Kling, X. Tan, W. Jo, H.-J. Kleebe, H. Fuess, and J. Rödel, J. Am. Ceram. Soc. **93**, 2452 (2010).